Physical Interpretation of the Phase Asymmetry of a Slant-Path Transmission Matrix

Neil J. McEwan, Zainol A. Abdul Rashid, *Student Member, IEEE*, and Stephen M. R. Jones

***Abstract*—The phase asymmetry of a 20-GHz slant-path transmission matrix during ice events is modeled in terms of two layers consisting of plate- and needle-type crystals. The microwave propagation data are consistent with the meteorological reports that the plate forms are usually predominant at higher altitudes than the needle forms.**

***Index Terms*—Electromagnetic propagation.**

I. Introduction

SWITCHED polarization transmissions of a satellite beacon provide the opportunity to measure the full transmission matrix of the atmospheric slant-path. Accurate and properly calibrated measurement of the matrix is important in modeling the populations of hydrometeors along the path. One effect revealed by careful calibration is asymmetry of the matrix. This paper discusses an interesting physical interpretation of phase asymmetry recently observed in ice events using the Olympus 20-GHz satellite beacon.

Using orthogonal linear basis polarizations, a symmetric matrix is observed when the path traverses either an arbitrary medium in which all particles have the same projected alignment or an arbitrary pure phase-shifting (lossless) medium in which the statistics of particle alignment remain constant along the path. At a high frequency such as 20 GHz, phase asymmetry of the matrix should be detectable and this will indicate the presence of differently aligned rain–ice or ice–ice particle populations along the path or more complex mixtures.

During ice events, the eigenpolarizations of the transmission matrix provide a measure of the mean projected orientation angles of the ice particles, which have a different characteristic behavior for needle and plate crystals. Any asymmetry of the matrix (which corresponds to eigenpolarizations becoming somewhat elliptical) is a measure of the homogeneity of the mean alignment along the path. This situation can be modeled (though not unambiguously) by a two-layer medium in which each layer has its own mean orientation direction.

The two most common types of ice particles at high altitudes are needle- and plate-type crystals. Knowledge of the occurrence and distribution of ice particles in clouds is not as satisfactory as that of water particles, owing to the difficulties of measurement and the variety of particle types. There is no generally accepted theoretical explanation of the observed concentrations and forms of ice crystals in clouds and of their growth by deposition of water vapor and other processes [1]. Summarizing studies of ice crystals reproduced in laboratories, Mason [2] indicated that the principal factor controlling the basic crystal habit is the temperature, but the secondary growth features are determined by the supersaturation. From several measurements made on real clouds, Srivastava [1] summarized the following pattern of ice crystal habit as a function of temperature: 1) $-3\,^{\circ}$C to $-8\,^{\circ}$C, needles; 2) $-8\,^{\circ}$C to $-25\,^{\circ}$C, plates, sector stars; 3) $-10\,^{\circ}$C to $-20\,^{\circ}$C, stellar dendrites; 4) less than $-20\,^{\circ}$C, prisms; and 5) less than $-30\,^{\circ}$C, clusters of hollow prisms. From the experimental and theoretical studies on ice crystal growth in supersaturated water vapor [3], [4], the mass growth rate (gram per second) of ice crystal is enhanced in the temperature range between $-3\,^{\circ}$C and $-21\,^{\circ}$C and is maximum at $-15\,^{\circ}$C. Heymsfield [5] also found that ice-particle concentrations at temperatures above $-15\,^{\circ}$C were 2–4 orders of magnitude higher than at lower temperature.

Since only gross shape can be resolved by microwave means, in this paper, we group all highly prolate forms (including columns and prisms) as "needles" and all highly oblate forms (including sector stars and stellar dendrites) as "plates." For propagation analysis, we expect the two main features to be a needle layer from $-3\,^{\circ}$C to $-8\,^{\circ}$C and a plate layer from $-8\,^{\circ}$C to $-20\,^{\circ}$C. It appears [2], [6] that "needles" would also appear at altitudes above the $-21\,^{\circ}$C level and "plates" below the $-3\,^{\circ}$C level, but in much lower concentrations.

Using a simplified ice model, we describe two methods of analysis that can reveal the existence of a two-layered ice medium along the path from the asymmetry of the transmission matrix.

II. Simplified Ice Model

In nature, ice crystals are found to fall with a preferred orientation due to aerodynamic and electrostatic forces. Under aerodynamic force, plate-type crystals fall in a horizontal plane with their short axis vertical and needle-type crystals fall with their long axis horizontal [7], [8]. For needles in this state, it appears that only a small force would be needed to influence the azimuth of the long axis and it is reasonably certain that both wind shears and horizontal components of electrostatic fields can produce a high degree of systematic alignment of needle azimuths. The relative dominance of these forces is uncertain, as is also the extent to which a common needle azimuth exists over the large volume that affects a microwave link, even if a high degree of azimuth alignment exists locally.

Manuscript received April 4, 1996; revised December 2, 1997.

The authors are with the Department of Electronic and Electrical Engineering, University of Bradford, West Yorkshire, BD7 1DP, U.K.

Publisher Item Identifier S 0018-926X(98)02741-0.

For an ideal population of ice-plates lying in the azimuth plane, the characteristic polarizations will be linear—vertical and horizontal. For an ideal population of ice-needles where all particles have the same long-axis azimuth, one eigenpolarization lies in the plane which contains the long-axis direction and the slant-path and this can range over all linear polarizations as the preferred azimuth varies. Such ideal behavior must be complicated by some coexistence of needles and plates in a given volume by incomplete control of needle azimuth by wind shear or electrostatic fields and possibly by domains of different needle azimuth caused by turbulent structure. However, it is a reasonably safe conclusion that the eigenpolarizations remain close to vertical and horizontal in mainly plate populations and are very much more variable (though still almost linear) in mainly needle populations. This is a sufficient condition for the following analysis.

III. Matrix Method

The following discussion uses transmission matrices $[T]$ referred to horizontal (x) and vertical (y) polarization, which are defined as forming a right-handed set when the z axis is the propagation direction from the satellite to the receiver. After removal of the clear-sky loss (free-space loss plus the gaseous absorption) and clear sky phase shift, matrix $[T]$ is defined by

$$\begin{bmatrix} E_x \\ E_y \end{bmatrix}_R = \begin{bmatrix} T_{xx} & T_{xy} \\ T_{yx} & T_{yy} \end{bmatrix} \begin{bmatrix} E_x \\ E_y \end{bmatrix}_T \tag{1}$$

where subscripts T and R denote transmitted and received field components respectively. $[T]$ is a unit matrix in clear weather.

We shall now assume two idealized layers—one with plates always exhibiting vertical and horizontal linear eigenpolarizations and a needle layer with much more variable linear eigenpolarizations. The transmission matrices for the plate layer $[P]$ and needle layer $[N]$ then take the forms of

$$[P] = \begin{bmatrix} 1 & 0 \\ 0 & e^{j\psi_p} \end{bmatrix}, \qquad [N] = \begin{bmatrix} A & X \\ X & B \end{bmatrix} \tag{2}$$

where ψ_p is the differential phase shift of the plate layer. (As overall phase shift cannot usually be measured in a beacon experiment, for convenience, T_{xx} has been set to unity for $[P]$ and $\arg(A)$ can also be forced to zero). The plate layer will produce excess phase lag for horizontal polarization so that $\psi_p > 0$. $|X|$ increases with both the tilt of the needle eigenpolarization and the total differential phase shift in the needles.

For a two-layer ice medium, the measured matrix can be expressed as (3) if the needle layer is at the higher altitude and as (4) when the plate layer is higher:

$$\begin{aligned} [T]_{pn} &= [P][N] \\ &= \begin{bmatrix} 1 & 0 \\ 0 & e^{j\psi_p} \end{bmatrix} \begin{bmatrix} A & X \\ X & B \end{bmatrix} \\ &= \begin{bmatrix} A & X \\ Xe^{j\psi_p} & Be^{j\psi_p} \end{bmatrix} \end{aligned} \tag{3}$$

or

$$\begin{aligned} [T]_{np} &= [N][P] \\ &= \begin{bmatrix} A & X \\ X & B \end{bmatrix} \begin{bmatrix} 1 & 0 \\ 0 & e^{j\psi_p} \end{bmatrix} \\ &= \begin{bmatrix} A & Xe^{j\psi_p} \\ X & Be^{j\psi_p} \end{bmatrix}. \end{aligned} \tag{4}$$

The asymmetry of the medium matrix can then be inspected from the ratio of the crosspolar terms. Results will be presented in terms of the differential crosspolar phase $(DXPH)$, which is defined as $\arg(T_{xy}/T_{yx})$. Our essential prediction is that $DXPH$ will be predominantly positive when plate crystal forms are dominant at higher altitudes.

It may also be noticed that the total differential copolar phase $(DCPH)$ (defined as $\arg(T_{yy}/T_{xx})$) is given by $\psi_p + \arg(B/A)$. Hence, although the contributions of the two layers to $DCPH$ can vary independently, a positive statistical correlation between $DCPH$ and $DXPH$ is expected when plates are uppermost.

IV. Eigenpolarization Analysis

An elegant alternative method of analysis considers the eigenpolarizations of the matrix. In the simple matrix analysis previously described, $DXPH$ becomes ill defined for small values of X, which can occur even for a strong event if its eigenpolarizations approach vertical/horizontal. However, the eigenpolarizations of a strong event remain equally well defined when X is negligible.

The characteristics of a lossless ice medium can be described by the three parameters τ, ϵ, and ψ, where τ represents the orientation or tilt angle of one eigenpolarization, ϵ defines its ellipticity with $\tan\epsilon$ equal to the axial ratio, and ψ the differential phase shift between the two eigenpolarizations of the medium.

Before treating a two-layer model, it is essential to state the sign conventions clearly. Here, we use a convention that τ measures the angle between horizontal polarization and the long axis of the polarization ellipse of the eigenpolarization that has excess phase *lag*. Following [9], increasing τ is defined as a counterclockwise (CCW) rotation of this long axis when looking toward the satellite. Parameter ϵ is defined for the eigenpolarization which has excess lag and is defined as positive when representing a left-handed elliptical polarization, i.e., one for which the electric field at a fixed point in space rotates clockwise (CW) when looking toward the satellite. The excess phase lag of the given eigenpolarization is represented by a positive value of the differential phase shift ψ.

A normal rain medium thus has τ and ϵ approximately zero and $\psi > 0$. To avoid a nonunique representation of a medium that has excess phase lag near vertical, we require that ψ remains positive, but allow $|\tau|$ to exceed 45°.

A simple method of constructing an eigenvector of the matrix $[N][P]$ is as follows. The matrices $[P]$ and $[N]$ are both symmetric and unitary and, therefore, their inverses are also their complex conjugates. Their square roots and inverses can be found by, respectively, halving or changing the sign

of the differential phase shifts that generate them. These new matrices are obviously also symmetric and unitary.

Let $\boldsymbol{u}$ and $\boldsymbol{u}^*$ denote a column vector and its conjugate. If $\boldsymbol{u}$ represents a given polarization, then $\boldsymbol{u}^*$ represents the polarization with the same tilt and ellipticity, but with the opposite sense of rotation.

Hence, in the special case where $\boldsymbol{u}$ represents a linear polarization, $\boldsymbol{u}^*$ must represent the same polarization so that $\boldsymbol{u} = \lambda \boldsymbol{u}^*$ for some complex number λ (of modulus unity).

Now let $\boldsymbol{m}$ be one of the infinite set of polarizations such that $[P]^{1/2}\boldsymbol{m}$ is a linear polarization. Then

$$\begin{aligned}[P]\boldsymbol{m} &= [P]^{1/2}([P]^{1/2}\boldsymbol{m}) = \lambda[P]^{1/2}([P]^{1/2}\boldsymbol{m})^* \\ &= \lambda[P]^{1/2}[P]^{1/2*}\boldsymbol{m}^* = \lambda[I]\boldsymbol{m}^* = \lambda\boldsymbol{m}^*. \end{aligned} \tag{5}$$

Vector $\boldsymbol{m}$ can now be restricted to only two possible values (which are orthogonal) by requiring that $[N]^{-(1/2)}\boldsymbol{m}$ is also a linear polarization. Since by a similar argument $[N]^{-1}\boldsymbol{m} = \mu\boldsymbol{m}^*$ for some number μ and $[N]\boldsymbol{m}^* = \mu^*\boldsymbol{m}$, it is easily shown that $\boldsymbol{m}$ is an eigenvector of $[N][P]$

$$[N][P]\boldsymbol{m} = [N]\lambda\boldsymbol{m}^* = \lambda\mu^*\boldsymbol{m}. \tag{6}$$

It has thus been shown that an eigenvector of $[N][P]$ must be expressible as $[P]^{-(1/2)}\boldsymbol{q}$ for a vector $\boldsymbol{q}$, which represents a linear polarization. Now if $\boldsymbol{q}$, which can be chosen to be real, is expressed in terms of its components q_x, q_y, the components of eigenvector $\boldsymbol{m}$ are given by

$$\begin{aligned}\begin{bmatrix} m_x \\ m_y \end{bmatrix} &= [P]^{-(1/2)}\begin{bmatrix} q_x \\ q_y \end{bmatrix} \\ &= \begin{bmatrix} 1 & 0 \\ 0 & e^{-j(\psi_p/2)} \end{bmatrix}\begin{bmatrix} q_x \\ q_y \end{bmatrix} \\ &= \begin{bmatrix} q_x \\ q_y e^{-j(\psi_p/2)} \end{bmatrix}. \end{aligned} \tag{7}$$

It is now clear that a positive ratio q_y/q_x corresponds to a positive value of τ. However, it also implies that the y component is lagging the x component and, hence, that the polarization ellipse has a CCW rotation and negative ϵ. It is therefore deduced that a positive value of τ will correspond to a negative value of ϵ if the plate layer lies above the needles and to a positive ϵ if the layers are interchanged.

The above algebraic operations can also be easily visualised using the Poincaré sphere, as in Figs. 1 and 2. In this representation, the cardinal points and equator should be viewed as a fixed coordinate system with respect to which all points (except the eigenpolarizations) are moved by the effect of the medium. A differential phase shift ψ between two orthogonal eigenpolarizations corresponds to a rotation of all points on the sphere through an angle ψ about a diameter passing through the points that represent the two eigenpolarizations.

A differential attenuation between two orthogonal eigenpolarizations causes any point on the sphere to move along the great circle, which connects it to the two eigenpolarizations. Finally, if the initial polarization is modified by a medium, the cross-polar discrimination (XPD) in decibels is given by $20\log_{10}\tan(\varphi/2)$, where φ is the great circle angle between the original polarization and its new position.

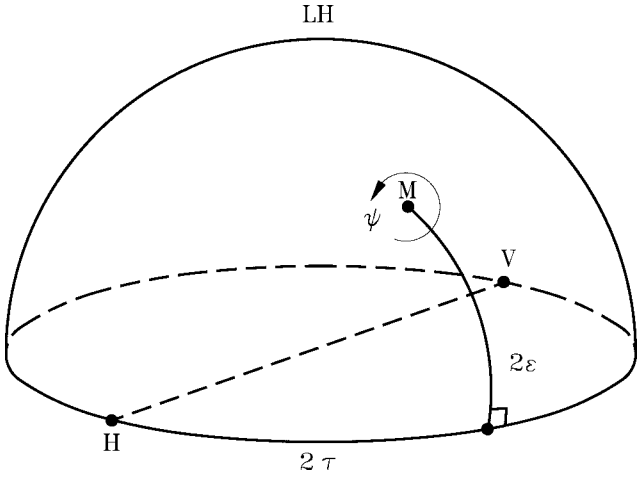

Fig. 1. Poincaré sphere representation.

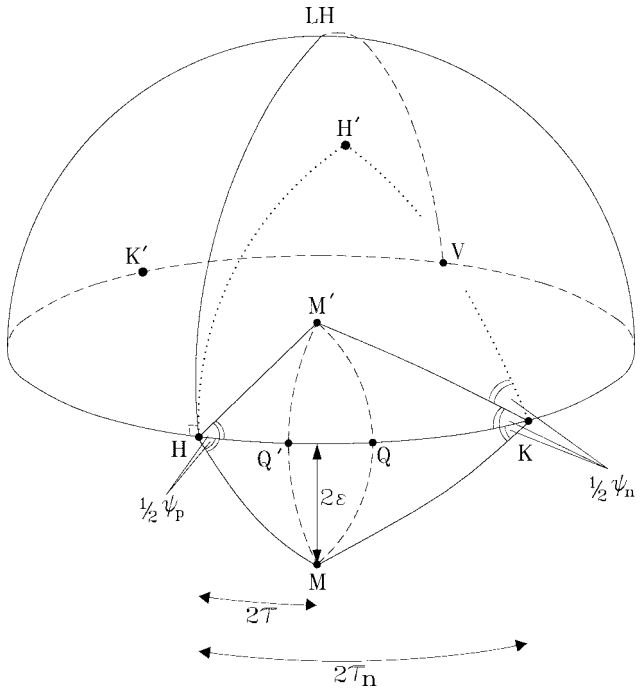

Fig. 2. Graphical representation of two population ice on a Poincaré sphere.

Fig. 1 shows the general transformation produced by a lossless medium using the three parameters τ, ϵ, and ψ previously defined. In Figs. 1 and 2, a medium with $\tau = 0$ is described by a CCW rotation of points on the sphere about axis HV when looking from H toward V.

The simplified two-population ice model is now considered, with the plate-type medium above the needle-type medium. First, the signal passes through a population of plate-type ice crystals whose effect is represented in Fig. 2 as a rotation R_p of the sphere through an angle ψ_p about the equatorial axis HV since τ_p is assumed zero. Then, as the signal passes through the population of needle-type ice crystals, there is a second rotation R_n of the sphere through angle ψ_n about the axis KK' defined by the needle eigenpolarization at angle τ_n. The required eigenpolarization M can now be found, as shown, at the intersection point of two great circles which

make angles $\psi_p/2$ and $\psi_n/2$ with the points H and K, respectively. Rotation R_p moves the point initially at M to M' along the path MQM'; R_n then moves it back to M along the path $M'Q'M$. Polarizations M, Q correspond to the column vectors $\boldsymbol{m}, \boldsymbol{q}$ defined above. Q' and Q are the linear polarizations obtained as $R_p^{1/2}(M)$ and $R_n^{-(1/2)}(M)$, as previously described in matrix notation. Clearly, M' is the required eigenpolarization when R_n and R_p are performed in the reverse order, and ψ can be constructed on the sphere as angle $H'M'H$, where polarization H' is chosen so that $R_n(H') = H$.

We again reach the conclusion that for the eigenpolarization with excess lag, ϵ will have the opposite sign to τ when the plate layer is uppermost, but the same sign if the layers are interchanged. With variable combinations of layers, a negative statistical correlation between ϵ and τ is predicted when plates are predominantly above needles and positive correlation if the reverse holds.

V. Results

The full slant-path transmission matrix was obtained using the 20-GHz switched polarization beacon transmitted from the Olympus satellite. The receiving station at Sparsholt, U.K., was operated by the Radio Communications Research Unit of Rutherford Appleton Laboratory. Details of the Olympus propagation experiment can be obtained from [10] and the Sparsholt station parameters are outlined in [11]. We have developed calibration methods [12] for these data which are believed to yield matrix measurements where the intrinsic amplitude and phase errors of all terms relative to the horizontal copolar channel are better than ± 0.2 dB and $\pm 5°$ and the crosspolar error terms have been mostly reduced to better than -45 dB by our matrix correction procedure. The phase calibration of the matrix has been described earlier [11], [12].

As the beacon polarizations appear tilted at the receiving site, the measured matrix has been mathematically rotated in the data analysis to refer it to horizontal and vertical basis polarizations. The geometrically calculated polarization tilt angle looking toward the satellite was 13.7° CW from vertical, but a value of 13.2° was inferred from the data analysis [12] and used to rotate the matrix. Eigenvectors of the matrix were calculated directly and the parameter ψ was obtained as the phase difference of the eigenvalues. ψ approximates to $DCPH$ when τ is fairly small.

A total of about 35 h of good ice events were measured from November 1992 to July 1993 and about 3 h of pure rain events were selected for comparison. Median values of 100 logger samples (i.e., with 10 s smoothing) are used in the data analysis.

Using the matrix analysis described earlier, an indication of two-layered ice particles can simply be inferred from the $DXPH$ parameter. The data sample density-gram of $DXPH$ versus ψ for the ice events is shown in Fig. 3. The limit of $XPD \leq 30$ dB is used to ensure that $DXPH$ is well defined. It can be seen from the figure that there is a very strong bias in the density toward positive values of $DXPH$ and also evidence of a positive correlation of $DXPH$ and ψ. This indicates that the plates are indeed at a higher altitude than the needles. The strength of the effect suggests that the separation of the two particle populations is rather well defined.

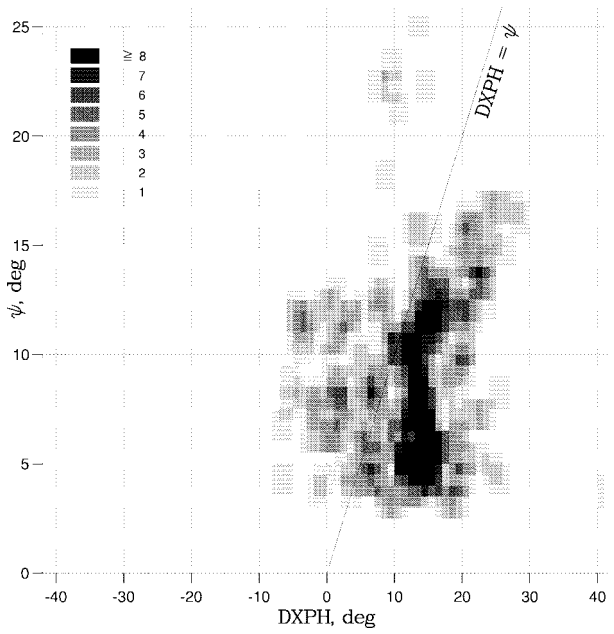

Fig. 3. Density-gram of $DXPH$ versus ψ for ice data with a limit of $XPD \leq 30$ dB. The figures use 10-s data samples. The grey scale value N is the number of data points lying in a window of width 3° in $DXPH$ and 1.5° in ψ. The peak value of N is 16 at $DXPH = 15°$ and $\psi = 5°$.

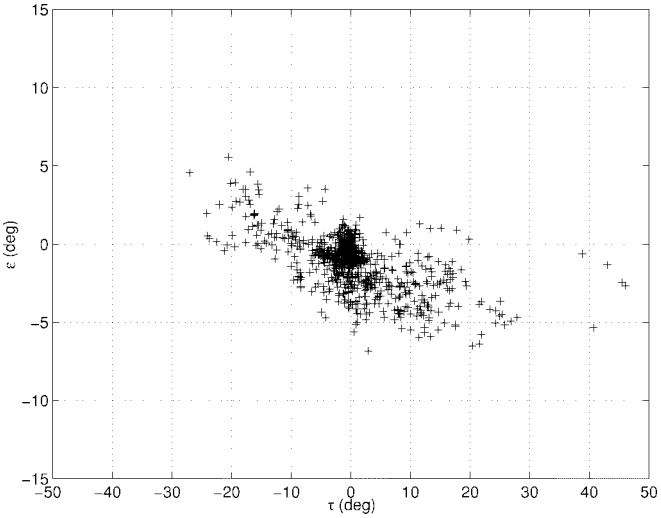

Fig. 4. Scattergram of τ versus ϵ for ice data with a limit of $\psi \geq 7.5°$.

A clear indication can also be found from the eigenpolarization representation. Fig. 4 shows a scattergram of τ versus ϵ, again selecting strong ice events by using a limit of $\psi \geq 7.5°$ to ensure well defined eigenpolarizations. The clear systematic negative correlation of τ and ϵ agrees with the prediction made in Section IV and confirms the earlier result from the simple matrix method that plate particles are mainly at the top.

A histogram of τ alone, as shown in Fig. 5, is sufficient to suggest the existence of the two populations of ice particles. It can be seen from the figure that there is a very strong concentration of data points at τ near zero, which indicates the dominant population of plate particles. However, the marked

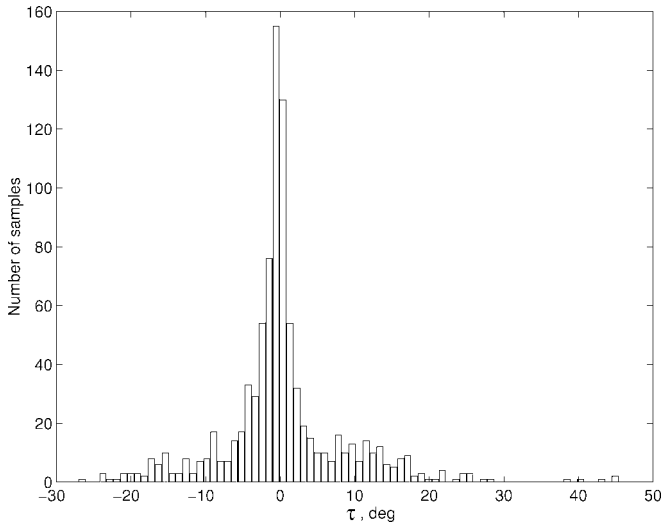

Fig. 5. Histogram of τ for ice data with limit of $\psi \geq 7.5°$.

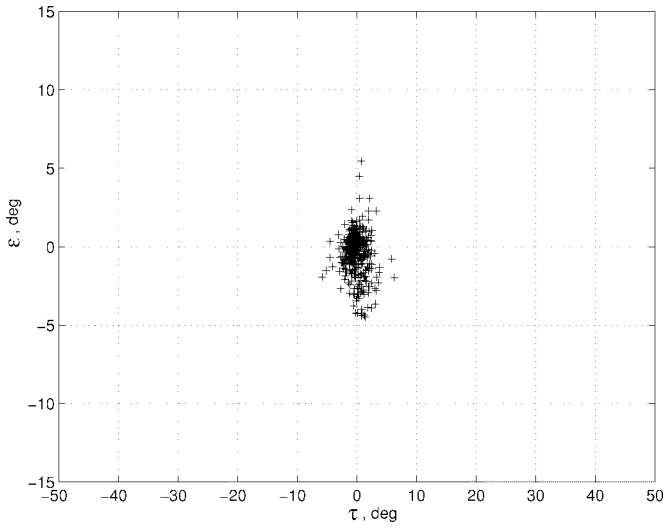

Fig. 6. Scattergram of τ versus ϵ for rain data with limit of $\psi \geq 7.5°$

tails of the distribution suggest a quite distinct population of needles producing a large effect on τ at times when the plate layer is tenuous. Interestingly the positive tail has a larger area than the negative.

Referring again to Fig. 3, a further interesting deduction can be made. The majority of data points lie to the right of the line $DXPH = \psi$. This implies that the needle population most commonly produces differential phase shift in opposition to that produced by the plates, i.e., the needle eigenpolarization with excess lead is generally nearer to horizontal than to vertical $(45° < \tau_n < 135°)$. For this to occur, the needle azimuths must be close to the azimuth of the link path (with τ_n near 90°) for a major fraction of the time. The conclusion is reinforced by noting that azimuths broadside to the link (τ_n near 0°) would produce ψ_n larger by a factor of about cosec^2 (elevation), equal to 4.2 for this slant-path, than would azimuths aligned with that of the link. (This is assuming highly prolate Rayleigh scatterers.) Hence, if needles were fully aligned, but with equiprobable azimuths, a majority of points to the left of the $DXPH = \psi$ line would be expected. A workable hypothesis is that the needles are mainly aligned north–south, broadside to a wind shear. (Prevailing winds are westerly at this site.) The satellite lies to the west of the site at azimuth 202° from north. Needles aligned exactly north–south give $\tau_n \approx +50°$ in this geometry. Coexisting with plates they would give a smaller positive τ. This could account for the larger positive tail in Fig. 5.

Finally, we present a scatterplot of τ versus ϵ from selected "pure rain" events using a limit of $\psi \geq 7.5°$, as shown in Fig. 6. The concentration of points near $\tau = \epsilon = 0°$ is in agreement with the rain cross-polarization theory where the canting angle of rain aloft is close to zero and its eigenpolarizations are linear vertical and horizontal [13]. These data are included as evidence that our calibration and analysis procedures are yielding very accurate values of ϵ and τ.

VI. Conclusion

The phase asymmetry of a slant-path transmission matrix seems to have previously received little attention from propagation investigators, but it contains interesting physical information. Our analysis of ice events reveals a surprisingly strong and systematic effect which supports reports from cloud physics sources [1]–[6] that plates are dominant at higher altitudes than needles; the data clearly show that for needles to lie above plates is a rare event. This is believed to be the first confirmation of this finding by a "remote" radio method. The novel method of analysis makes it possible to see, for the first time, separate cross-polarizing contributions from two ice-particle types; for the Sparsholt link geometry, it reveals a systematic tendency for these contributions to cancel.

It is likely that similar evidence can be obtained by radar methods and various approaches have been suggested [14]–[16]. The radio-link analysis lacks the spatial resolution of a radar, but has the interesting feature of yielding a measurement with D^3 size weighting. A radar measurement with this weighting can be obtained by analyzing differential phases from gate to gate, but this method does not yet seem to have been developed to the point of clearly resolving particle types.

Maekawa [17] (using data obtained in Japan) shows that the radar echoes correlating most strongly with beacon cross-polarization occur around the -15 °C height, which is also the height of most rapid particle formation [3]–[5]. Maekawa also infers from this height that they are mainly of plate-type origin. He postulates that these particles coalesce rapidly and, thus, lose anisotropy as they fall so that they no longer contribute to the link cross polarization. For the Sparsholt site, the analysis of asymmetry and eigenpolarizations indicates a weaker, but not negligible, effect from needle crystals forming at lower altitudes. Ice cross polarization at this site is consistent with a model where a layer consisting almost entirely of plate crystals, with very little variation of tilt, lies above a layer consisting mainly of needles; these must be assumed to have long axes preferentially aligned along azimuths close to north–south.

Viewed as a remote sensing tool, the beacon experiment has the potential to yield a direct estimate of integrated ice-water content (IWC) along the path. It has the D^3

weighting needed to avoid size distribution modeling errors. The present analysis shows that at many sites, simple inference of IWC from XPD would be a considerable underestimate because of systematic cancellation. However, using the two-layer model derived from the matrix, the contributions can be assessed separately using different constants of proportionality between ψ and IWC for the two basic crystal forms. A complete transmission matrix yields the three real parameters ψ_p, ψ_n, and τ_n needed to fully specify this ice model, but only if measurements are properly calibrated. With the very simple assumptions made here, the needle matrix $[T]_n$ can be found by right multiplying ("deplating") the measured ice matrix $[T]$ by the inverse of the plate matrix $[T]_p^{-1}$. This is trivially found since ψ_p is just equal to the $[T]$ matrix $DXPH$. A final word of caution is needed since, according to Maekawa's picture, there is likely to exist substantial ice content in coalesced plates that are invisible to the cross-polar measurement. Possibly, a development of the model including fall and coalescence would allow their contributions to IWC to be estimated indirectly from the plate parameter ψ_p or from a concurrent radar measurement.

ACKNOWLEDGMENT

The authors would like to thank the Radio Communications Research Unit of Rutherford Appleton Laboratory (RAL), U.K., for providing them with the Sparsholt propagation data.

REFERENCES

[1] R. C. Srivastava, "The cloud physics of particle size distributions—A review," *J. Res. Atmosph.*, vol. 8, pp. 23–39, 1974.
[2] B. J. Mason, *The Physics of Clouds*. London, U.K.: Oxford Univ. Press, 1971.
[3] L. R. Koenig, "Numerical modeling of ice deposition," *J. Atmosph. Sci.*, vol. 28, pp. 226–237, 1971.
[4] B. F. Ryan, E. R. Wishart, and D. E. Shaw, "The growth rates and densities of ice crystals between -3 °C and -21 °C," *J. Atmosph. Sci.*, vol. 33, pp. 842–850, 1976.
[5] A. J. Heymsfield, "Precipitation development in stratiform ice clouds: A microphysical and dynamical study," *J. Atmosph. Sci.*, vol. 34, pp. 367–381, 1977.
[6] H. R. Pruppacher and J. D. Klett, *Microphysics of Clouds and Precipitation*. Dordrecht, Holland: Riedel, 1980.
[7] J. P. Mon, "Backward and forward scattering of microwaves by ice particles: A review," *Radio Sci.*, vol. 17, pp. 953–971, 1982.
[8] D. P. Haworth, N. J. McEwan, and P. A. Watson, "Crosspolarization for linearly and circularly polarized waves propagating through a population of ice particles on satellite-earth paths," *Electron. Lett.*, vol. 13, pp. 703–704, 1977.
[9] J. D. Kraus, *Antennas*, 2nd ed. New York: McGraw-Hill, 1988.
[10] B. R. Arbesser-Rastburg and G. Brussaard, "Propagation research in Europe using the Olympus satellite," *Proc. IEEE*, vol. 81, pp. 865–875, June 1993.
[11] N. J. McEwan, Z. A. Abdul Rashid, and S. M. R. Jones, "Phase calibration of Olympus 20 GHz switched polarization satellite beacon," *Electron. Lett.*, vol. 31, pp. 950–951, 1995.
[12] ———, "Calibration techniques for Olympus 20-GHz switched polarization satellite beacon measurements," *IEEE Trans. Antennas Propagat.*, vol. 44, pp. 1266–1276, Sept. 1996.
[13] G. Brussaard, "A meteorological model for rain-induced crosspolarization," *IEEE Trans. Antennas Propagat.*, vol. AP-24, pp. 5–11, Jan. 1976.
[14] J. Vivekanandan and W. M. Adams, "Theoretical investigation of multiparameter radar scattering characteristics of ice crystals," in *26th Int. Conf. Radar Meteorol. Amer. Meteorol. Soc.*, Norman, OK, May 1993, pp. 109–111.
[15] K. F. Evans and J. Vivekanandan, "Multiparameter radar and microwave radiative transfer modeling of nonspherical atmospheric ice particles," *IEEE Trans. Geosci. Remote Sensing*, vol. 28, pp. 423–437, July 1990.
[16] C. Tang and K. Aydin, "Scattering from ice crystals at 94- and 220-GHz millimeter wave frequencies," *IEEE Trans. Geosci. Remote Sensing*, vol. 33, pp. 93–99, Jan. 1995.
[17] Y. Maekawa, N. S. Chang, and A. Miyazaki, "Ice depolarizations on Ka band (20 GHz) satellite-to-ground path and correlation with radar observations," *Radio Sci.*, vol. 28, pp. 249–259, 1993.

Neil J. McEwan was born in London, U.K., in 1948. He received the B.A. degree in mathematics from the University of Cambridge, U.K., in 1969, and the Ph.D. degree in radio astronomy from the University of Manchester, U.K., in 1975.

He is currently Reader in Electromagnetics in the Department of Electronic and Electrical Engineering, University of Bradford, U.K., which he joined as a Research Fellow in 1972. He has previously worked on microwave propagation in the troposphere and was involved in propagation experiments using the ATS-6 and European OTS satellites. In 1987 he was with the Millitech Corporation, South Deerfield, MA, as Visiting Research Scientist.

Dr. McEwan is a member of the Institution of Electrical Engineers.

Zainol A. Abdul Rashid (S'95) received the B.Sc. degree in electronics from Universiti Kebangsaan Malaysia (UKM), Malaysia, in 1985, the M.Sc. degree in microprocessor engineering from the University of Bradford, U.K., in 1987, and the Ph.D. degree in microwave propagation from the University of Bradford, U.K., in 1997

Since 1989, he has been a member of the Faculty of Engineering, UKM.

Stephen M. R. Jones received the B.A. degree in physics (honors) from the University of East Anglia, Norwich, U.K., in 1975, and the Ph.D. degree from the University of Bradford, U.K., in 1993.

He is currently a Lecturer in the Department of Electronic and Electrical Engineering, University of Bradford, U.K. He joined that department's microwave and millimeter-wave propagation team in 1987 and has since worked on a number of research projects including development of a 10-GHz bistatic-scatter link and a study of scintillation on 11/14 GHz slant-paths. He was a member of the U.K. Olympus Propagation Experimenters Group (OPEG-UK). His current interests include Ka-Band satellite-mobile radio, and millimeter-wave multichannel distribution systems (MMDS), microcellular, and indoor propagation.